Inorganic Chemistry

Communication

pubs.acs.org/IC

Polyoxometalate-Supported 3d−4f Heterometallic Single-Molecule Magnets

Xiaojia Feng,[†] Wenzhe Zhou,[†] Yangguang Li,*[,†] Hongshan Ke,[‡] Jinkui Tang,*[,‡] Rodolphe Clérac,*[,§,⊥] Yonghui Wang,[†] Zhongmin Su,[†] and Enbo Wang[†]

[†]Key Laboratory of Polyoxometalate Science of Ministry of Education, Faculty of Chemistry, Northeast Normal University, Changchun 130024, People's Republic of China

[‡]State Key Laboratory of Rare Earth Resource Utilization, Changchun Institute of Applied Chemistry, Chinese Academy of Sciences, Changchun 130022, People's Republic of China

[§]CNRS, CRPP, UPR 8641, Centre de Recherche Paul Pascal (CRPP), Equipe "Matériaux Moléculaires Magnétiques", 115 avenue du Dr. Albert Schweitzer, Pessac F-33600, France

[⊥]Univ. de Bordeaux, CRPP, UPR 8641, Pessac F-33600, France

Supporting Information

ABSTRACT: The reactions of $[CuTbL_{Schiff}(H_2O)_3Cl_2]Cl$ complexes with A- or B-type Anderson polyoxoanions lead to new polyoxometalate-supported 3d−4f heterometallic systems with single-molecule-magnet behavior.

Polyoxometalates (POMs) are unique nanosized complexes with oxygen-rich surfaces and controllable size, shape, and charge. In the past few years, these molecular objects have been considered as inorganic ligands to assemble various transition-metal (TM) or lanthanide (Ln) ions into aggregates with interesting magnetic properties such as single-molecule-magnet (SMM) behavior.[1−5] In this research field, several POM-based SMMs or SMMs decorated by POM ligands have been reported.[4] Furthermore, the hybrid POM materials behaving as SMMs have also been prepared by dispersing high-spin anisotropic units (like SMMs) into the porous anionic POM-based structures.[5] A recent aspect of this research field has focused on the construction of new POM-supported molecular aggregates assembled by high-spin and anisotropic 3d−4f heterometallic complexes.[6] Until now, only a few examples have been reported,[7] but none of them exhibits SMM properties. During the self-assembly process, a competition between reactions involving the polyoxoanions and both Ln and TM ions occurs in an uncontrollable manner. In most of the synthetic conditions, the obtained species are not the ones expected.[8]

On the basis of the above consideration, we attempt to explore new systems that can combine various 3d−4f heterometallic complexes with POMs. The $\{TM^{II}Ln^{III}L\}^{n+}$ dinuclear complexes assembled by different Schiff-base ligands (L)[9] appear to be ideal candidates to validate our synthetic strategy (Scheme 1a). $\{TM^{II}Ln^{III}L\}^{n+}$ complexes are available with many different TM and Ln centers, and their coordinating counteranions, usually NO_3^- or Cl^-, can be substituted by various organic O- or N-donor ligands.[10] Thus, it is possible to combine $\{TM^{II}Ln^{III}L\}^{n+}$ units (especially the potential $\{Cu^{II}Tb^{III}\}$ SMM moiety) with various polyoxoanions. Herein, we report two new POM-supported 3d−4f heterometallic compounds, $[\{CuTbL(H_2O)_3\}_2\{IMo_6O_{24}\}]Cl\cdot 2MeOH\cdot 8H_2O$ (**1**) and $[\{CuTbL(H_2O)_2\}_2\{AlMo_6O_{18}(OH)_6\}_2]\cdot MeOH\cdot 10H_2O$ (**2**) [L = *N*,*N*′-bis(3-methoxysalicylidene)-ethylenediamine]. In these new molecular systems, the coordination environment and assembly mode of {CuTb} units are modulated by different Anderson-type POM complexes (Scheme 1b). More interestingly, both compounds exhibit SMM behaviors, which is not observed in their precursor $[CuTbL(H_2O)_3Cl_2]Cl\cdot MeOH$ (**3**).

Scheme 1. Schematic View of (a) a $\{TM^{II}Ln^{III}\}$ Unit Based on a Schiff-Base Ligand and (b) an Anderson-Type POM ($O_c = O^{2-}$ or OH^- for an A- or B-Type Anderson POM, respectively)

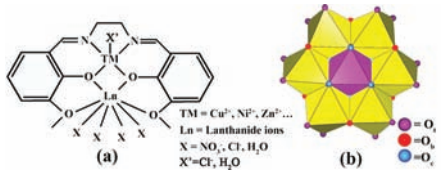

Red-brown block crystals of **1** and **2** were prepared by layering a methanol solution of $[CuTbL(H_2O)_3Cl_2]Cl$ onto an aqueous solution of A- or B-type Anderson POM complexes.[11] Both compounds crystallize in the triclinic space group $P\bar{1}$.[12] The crystal structure of **1** consists of two $[CuTbL(H_2O)_3]^{3+}$ moieties and one A-type Anderson $[IMo_6O_{24}]^{5-}$ polyoxoanion[13a] (Figures 1 and S1 in the Supporting Information, SI). In the {CuTb} moieties, the Cu^{2+} center is five-coordinated with two imine N atoms, two phenolate O atoms, and one terminal methanol. The nine-coordinated Tb^{III} center adopts a capped square-antiprismatic geometry with nine O atoms: two phenolate, two ethoxy, two O_t atoms from POMs, and three water molecules. On the basis of the above coordination modes, two {CuTb} units are covalently linked to one POM moiety (Figure 1).

Received: November 9, 2011
Published: February 15, 2012

   dx.doi.org/10.1021/ic202418y | *Inorg. Chem.* 2012, 51, 2722−2724

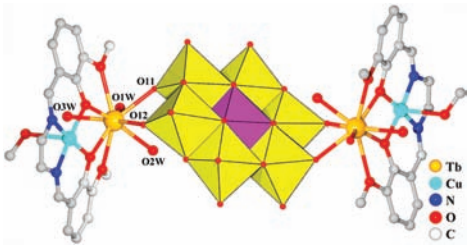

Figure 1. View of the molecular structure of **1**. The H atoms, Cl anions, and interstitial solvents are omitted for clarity.

Compound **2** is composed of two cationic $[CuTbL(H_2O)_2]^{3+}$ units and two B-type Anderson $[AlMo_6O_{24}H_6]^{3-}$ polyoxoanions[13b] (Figures 2 and S2 in the SI). Generally, both

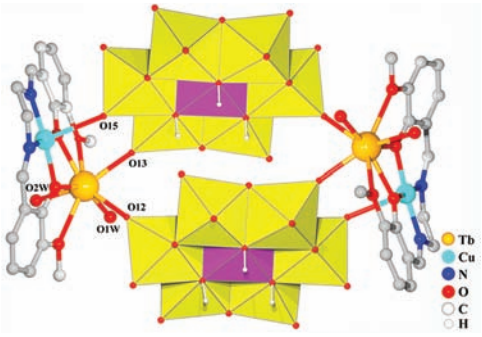

Figure 2. View of the molecular structure of **2**. The H atoms on organic ligands and interstitial solvent molecules are omitted for clarity.

A- and B-type Anderson POMs possess the same molecular structure, but the six O_c atoms in the B-type Anderson unit are OH^- groups,[13b] which induce less negatively charged species. In **2**, each Cu^{2+} center is five-coordinated with two imine N atoms, two phenolate O atoms, and one O atom (O15) from a polyoxoanion. The Tb^{III} center is eight-coordinated with four types of O atoms: two phenolate, two ethoxy, two O_t from different polyoxoanions, and two water molecules, showing a square-antiprismatic geometry. On the basis of the above coordination modes, two {CuTb} moieties are covalently connected with two B-type Anderson POM units, forming a ring-type POM-supported 3d−4f heterometallic complex (Figure 2).

It is worth mentioning that substitution of the donor anions, Cl^-, of the precursor **3** by POM ligands modulates the coordination environment of Tb centers and the structural parameters of the $\{CuO_2Tb\}$ units, such as the dihedral angle and the Cu···Tb distance (Figures S1−S4 and Tables S2 and S3 in the SI). Moreover, in the packing arrangement of **1** and **2**, each POM-supported {CuTb} complex adopts the same orientation and is well separated without strong hydrogen-bonding or $\pi-\pi$ interactions (Figures S5−S9 in the SI). The {CuTb} unit in **3** exhibits two different orientations, and the adjacent {CuTb} moieties possess extensive and strong H-bond interactions between Cl^- and coordinated water molecules (Figure S6 and Table S4 in the SI).

The direct-current (dc) magnetic susceptibilities of **1**, **2**, and their precursor **3** have been measured and are shown as χT vs T plots (Figures S18 and S19 in the SI). Compounds **1** and **2** exhibit similar behavior, with χT values at 300 K (22.2−22.3 cm^3 K mol^{-1}) that are slightly lower than expected (24.375 cm^3 K mol^{-1}) for two Cu^{2+} ($S = {}^1/_2$, $g = 2$) and two Tb^{III} ions ($^7F_6$, $J = 6$, $g_J = {}^3/_2$). The χT vs T plots (Figure S18 in the SI) suggest the coexistence of competitive phenomena: (i) the intrinsic Tb^{III} magnetism that is dominated by thermal depopulation of the 13 sublevels of the $^7F_6$ ground state (induced by the spin−orbit coupling and a low symmetry crystal field) explains the decrease of χT products below 300 K; (ii) the weak intramolecular Cu−Tb ferromagnetic interactions that are the origin of the χT product increase until 8 K;[14,15] (iii) finally, the presence of magnetic anisotropy brought about by the Tb ions and/or weak antiferromagnetic interactions between $\{CuO_2Tb\}$ complexes through weak intermolecular contacts or POM linkers explains the decrease of χT below 8 K. The χT vs T plot of the precursor **3** (Figure S19 in the SI) reveals a different thermal behavior. The room temperature χT value is 13.1 cm^3 K mol^{-1}, which is slightly higher than expected (12.18 cm^3 K mol^{-1}) for the noninteracting Cu^{2+} and Tb^{III} ions. Upon a lowering of the temperature from 300 K, the χT value increases rapidly to reach a maximum of 14.9 cm^3 K mol^{-1} at 14 K and then decreases to 13.8 cm^3 K mol^{-1} at 2 K. The observed difference of the magnetic properties between **3** and complexes **1** and **2** highlights a much stronger intramolecular ferromagnetic interaction in **3** and also likely a significant change of the intrinsic Tb^{III} magnetic properties induced by geometrical modifications of the Tb^{III} coordination sphere with different donor ligands (Tables S2 and S3 in the SI).

In alternating-current (ac) susceptibility measurements, the slow relaxation of magnetization is observed in **1** and **2** based on the appearance of out-of-phase signals (χ'') below 10 K (Figures 3 and S21 and S22 in the SI), suggesting SMM

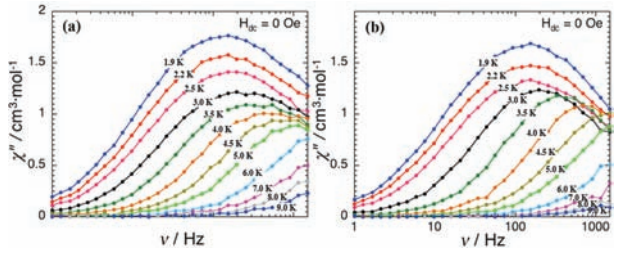

Figure 3. Frequency dependence of the imaginary (χ'') parts of the ac susceptibilities for **1** (a) and **2** (b) in zero dc field. Solid lines are guides for the eyes.

behavior.[15,16] From the frequency dependence of the ac data (Figure 3), the relaxation time, τ, of the systems has been estimated and plotted in a semilogarithmic scale as a function of T^{-1} (Figure S22 in the SI). τ is not following a simple Arrhenius law because τ is becoming temperature-independent below 2.5 K, as expected for a SMM in a pure quantum regime of relaxation. The characteristic time of the quantum tunneling of magnetization (QTM) is fast (ca. 1.1×10^{-3} s), explaining the absence of M vs H hysteresis at the sweeping rate used in a classical magnetometer. Therefore, the energy gap, Δ, associated with the thermally activated regime of relaxation has been estimated from the experimental data above 4 K. The energy gaps found are 17.1 and 20.8 K and the preexponential factors, τ_0, are about 4.0×10^{-6} and 1.1×10^{-6} s for **1** and **2**, respectively. It should be noticed that the τ_0 values are notably larger than the expected values of around $10^{-9}-10^{-11}$ s for SMMs. These values are obviously enhanced by the presence of QTM, suggesting that the obtained Δ must be taken as a lower limit of the real thermal energy gaps. It is also noteworthy that

dx.doi.org/10.1021/ic202418y | Inorg. Chem. 2012, 51, 2722−2724

the ac susceptibility measurements for the precursor **3** reveal the absence of slow relaxation of magnetization (Figure S20 in the SI). Such a magnetic difference between precursor **3** and compounds **1** and **2** is mainly attributed to two possible reasons: (i) when Cl^- is substituted by POM anions, the coordination sphere of Tb^{III} is modulated and then the anisotropy of Tb is enhanced, and/or (ii) the extensive intercomplex magnetic interaction in **3** is obviously shielded when POMs are introduced into the molecular system, revealing the intrinsic SMMs properties of the {CuTb} complex.[15,16]

In summary, the reaction of $\{CuTbL_{schiff}\}$ moieties with different Anderson-type POMs leads to the first two examples of Anderson-type POM-supported 3d−4f heterometallic complexes. In contrast to their $\{CuTbL_{schiff}\}$ precursor, compounds **1** and **2** exhibit slow relaxation of their magnetization observed by ac susceptibility measurements, demonstrating SMM properties. This work shows an easy-chemical way to synthesize POM-supported 3d−4f heterometallic SMMs. Moreover, the two compounds further illustrate how POMs could be used to assemble, isolate, and organize new SMM systems based on the coordination properties of the POM building blocks.

■ ASSOCIATED CONTENT

Supporting Information

X-ray crystallographic files (CIF), experimental details, crystallographic data, packing arrangement of **1**−**3**, IR, UV, XRD, TGA, and magnetism of **1**−**3**. This material is available free of charge via the Internet at http://pubs.acs.org.

■ AUTHOR INFORMATION

Corresponding Author

*E-mail: liyg658@nenu.edu.cn (Y.L.), tang@ciac.jl.cn (J.T.), clerac@crpp-bordeaux.cnrs.fr (R.C.).

Notes

The authors declare no competing financial interest.

■ ACKNOWLEDGMENTS

This work was supported by the National Natural Science Foundation of China (Grants 91027002 and 21131001), The National Grand Fundamental Research 973 Program of China (Grant 2010CB635114), the Fundamental Research Funds for the Central Universities, the Conseil Régional d'Aquitaine, the GIS Advanced Materials in Aquitaine (COMET Project), the Université of Bordeaux, the CNRS, and the ANR (NT09_469563, AC-MAGnets project).

■ REFERENCES

(1) Müller, A.; Peters, F.; Pope, M. T.; Gatteschi, D. *Chem. Rev.* **1998**, *98*, 239.

(2) Juan, J. M. C.; Coronado, E. *Coord. Chem. Rev.* **1999**, *193*, 361.

(3) Long, D. L.; Tsunashima, R.; Cronin, L. *Angew. Chem., Int. Ed.* **2010**, *49*, 1736.

(4) (a) AlDamen, M. A.; Clemente-Juan, J. M.; Coronado, E.; Martí-Gastaldo, C.; Gaita-Ariño, A. *J. Am. Chem. Soc.* **2008**, *130*, 8874. (b) AlDamen, M. A.; Cardona-Serra, S. J.; Clemente-Juan, M.; Coronado, E.; Gaita-Ariño, A.; Martí-Gastaldo, C.; Luis, F.; Montero, O. *Inorg. Chem.* **2009**, *48*, 3467. (c) Ritchie, C.; Ferguson, A.; Nojiri, H.; Miras, H. N.; Song, Y. F.; Long, D. L.; Burkholder, E.; Murrie, M.; Kögerler, P.; Brechin, E. K.; Cronin, L. *Angew. Chem., Int. Ed.* **2008**, *47*, 5609. (d) Compain, J. D.; Mialane, P.; Dolbecq, A.; Mbomekallé, I. M.; Marrot, J.; Sécheresse, F.; Rivière, E.; Rogez, G.; Wernsdorfer, W. *Angew. Chem., Int. Ed.* **2009**, *48*, 3077. (e) Fang, X. K.; Speldrich, M.; Schilder, H.; Cao, R.; O'Halloran, K. P.; Hill, C. L.; Kögerler, P. *Chem. Commun.* **2010**, *46*, 2760. (f) Ibrahim, M.; Lan, Y.; Bassil, B. S.; Xiang, Y. X.; Suchopar, A.; Powell, A. K.; Kortz, U. *Angew. Chem., Int. Ed.* **2011**, *50*, 4708. (g) Ritchie, C.; Speldrich, M.; Gable, R. W.; Sorace, L.; Kögerler, P.; Boskovic, C. *Inorg. Chem.* **2011**, *50*, 7004.

(5) Wu, Q.; Li, Y. G.; Wang, Y. H.; Clérac, R.; Lu, Y.; Wang, E. B. *Chem. Commun.* **2009**, 5743.

(6) (a) Rinck, J.; Novitchi, G.; Van den Heuvel, W.; Ungur, L.; Lan, Y.; Wernsdorfer, W.; Anson, C. E.; Chibotaru, L. F.; Powell, A. K. *Angew. Chem., Int. Ed.* **2010**, *49*, 7538. (b) Stamatatos, T. C.; Teat, S. J.; Wernsdorfer, W.; Christou, G. *Angew. Chem., Int. Ed.* **2009**, *48*, 521.

(7) (a) Merca, A.; Müller, A.; van Slageren, J.; Läge, M.; Krebs, B. *J. Cluster Sci.* **2007**, *18*, 711. (b) Chen, W. L.; Li, Y. G.; Wang, Y. H.; Wang, E. B.; Zhang, Z. M. *Dalton Trans.* **2008**, 865. (c) Fang, X. K.; Kögerler, P. *Angew. Chem., Int. Ed.* **2008**, *47*, 8123. (d) Fang, X. K.; Kögerler, P. *Chem. Commun.* **2008**, 3396. (e) Nohra, B.; Mialane, P.; Dolbecq, A.; Rivière, E.; Marrot, J.; Sécheresse, F. *Chem. Commun.* **2009**, 2703. (f) Reinoso, S.; Galán-Mascarós, J. R. *Inorg. Chem.* **2010**, *49*, 377. (g) Reinoso, S. *Dalton Trans.* **2011**, *40*, 6610.

(8) (a) Chen, W. L.; Li, Y. G.; Wang, Y. H.; Wang, E. B. *Eur. J. Inorg. Chem.* **2007**, 2216. (b) Chen, W. L.; Li, Y. G.; Wang, Y. H.; Wang, E. B.; Su, Z. M. *Dalton Trans.* **2007**, 4293.

(9) (a) Gheorghe, R.; Andruh, M.; Moller, A.; Schmidtmann, M. *Inorg. Chem.* **2002**, *41*, 5314. (b) Madalan, A. M.; Roesky, H. W.; Andruh, M.; Noltemeyer, M.; Stanica, N. *Chem. Commun.* **2002**, 1638. (c) Costes, J. P.; Novitchi, G.; Shova, S.; Dahan, F.; Donnadieu, B.; Tuchagues, J. P. *Inorg. Chem.* **2004**, *43*, 7792.

(10) (a) Gheorghe, R.; Cucos, P.; Andruh, M.; Costes, J. P.; Donnadieu, B.; Shova, S. *Chem.—Eur. J.* **2006**, *12*, 187. (b) Novitchi, G.; Wernsdorfer, W.; Chibotaru, L. F.; Costes, J. P.; Anson, C. E.; Powell, A. K. *Angew. Chem., Int. Ed.* **2009**, *48*, 1614.

(11) Synthesis of **1**: A solvent mixture (5 mL) of methanol and water (3:2, v/v) as a buffer layer was slowly layered onto an aqueous solution (2 mL) of $Na_5[IMo_6O_{24}]\cdot 3H_2O$ (12 mg, 0.01 mmol) in a test tube. Then, $[CuTbL(H_2O)_3Cl_2]Cl$ (15 mg, 0.02 mmol) in a 4 mL mixture of methanol and water (3:1, v/v) was slowly layered onto the buffer layer. The tube was sealed and left undisturbed at room temperature. After 2 weeks, the red-brown block crystals were isolated and collected by filtration (yield: 42% based on Mo). The synthesis of **2** is similar to that of **1**, except that $Na_3[AlMo_6O_{24}H_6]\cdot 3H_2O$ (24 mg, 0.02mmol) was used (yield: 75% based on Mo).

(12) Crystal data of **1** for $C_{38}H_{74}N_4O_{49}Cu_2Tb_2IMo_6Cl$, M_r = 2553.92, triclinic, space group $P\bar{1}$ with a = 9.7486(2) Å, b = 13.569(3) Å, c = 15.096(3) Å, α = 73.78(3)°, β = 74.36(3)°, γ = 79.65(3)°, V = 1834.6(7) Å^3; Z = 1; D_{calcd} = 2.312 g cm^{-3}; T = 150(2) K. The final refinement gave R1 = 0.0644, wR2 = 0.1767, and GOF = 1.023 for 14 210 observed reflections with $I > 2\sigma(I)$. Crystal data of **2** for $C_{37}H_{84}N_4O_{73}Cu_2Tb_2Al_2Mo_{12}$, M_r = 3403.24, triclinic, space group $P\bar{1}$ with a = 13.215(3) Å, b = 13.487(3) Å, c = 15.190(3) Å, α = 100.49(3)°, β = 99.61(3)°, γ = 108.88(3)°, V = 2443.5(9) Å^3; Z = 1; D_{calcd} = 2.313 g cm^{-3}; T = 150(2) K. The final refinement gave R1 = 0.0806, wR2 = 0.1993, and GOF = 1.046 for 17 958 observed reflections with $I > 2\sigma(I)$.

(13) (a) Filowitz, M.; Ho, R. K. C.; Klemperer, W. G.; Shum, W. *Inorg. Chem.* **1979**, *18*, 93. (b) Shivaiah, V.; Nagaraju, M.; Das, S. K. *Inorg. Chem.* **2003**, *42*, 6604.

(14) (a) Costes, J. P.; Dahan, F.; Dupuis, A. *Inorg. Chem.* **2000**, *39*, 165. (b) He, F.; Tong, M. L.; Chen, X. M. *Inorg. Chem.* **2005**, *44*, 8285.

(15) (a) Costes, J. P.; Dahan, F.; Wernsdorfer, W. *Inorg. Chem.* **2006**, *45*, 5. (b) Costes, J. P.; Auchel, M.; Dahan, F.; Peyrou, V.; Shova, S.; Wernsdorfer, W. *Inorg. Chem.* **2006**, *45*, 1924.

(16) (a) Osa, S.; Kido, T.; Matsumoto, N.; Re, N.; Pochaba, A.; Mrozinski, J. *J. Am. Chem. Soc.* **2004**, *126*, 420. (b) Kajiwara, T.; Nakano, M.; Takaishi, S.; Yamashita, M. *Inorg. Chem.* **2008**, *47*, 8604.